CrossMark

Studies on Dilute Magnetic Semiconducting Co-Doped CdS Thin Films Prepared by Chemical Bath Deposition method

S. Saravanakumar[1] · R. Chandramohan[1] · R. Premarani[2] · J. Jebaraj Devadasan[3] · J. Thirumalai[4]

Abstract The Co-doped CdS polycrystalline thin films were deposited onto the glass substrates by chemical bath deposition method. All the deposited films were characterized for structural, surface morphology, elemental, optical and magnetic properties using X-ray diffractometer, scanning electron microscopy (SEM), energy dispersive X-ray, UV–Vis. NIR spectrometer and Vibrating sample magnetometer before and after doping. The thin films exhibit hexagonal wurtzite structure with (0 0 2) preferential orientation and the calculated crystallite size is 29 and 18 nm for pristine and Co-doped CdS films respectively. X-ray photoelectron spectroscopy (XPS) analysis showed the presence of Cd, S and Co peaks along with O 1s peak. The studies revealed that the surface Cd atoms of films are found to be bound either to S atoms or O atoms. SEM images showed grainy surface for pristine which gets modified under Co doping. Energy dispersive analysis using X-rays confirmed the presence of Cd, S and Co in the films. From optical transmittance spectra, the bandgap was estimated and found to be varying from 2.4 to 2.27 eV with the increase of Co concentrations. The room-temperature ferromagnetic behavior was exhibited by Co-doped CdS films.

1 Introduction

Currently, renewed interests are observed at room-temperature ferromagnetic (FM) semiconductors for spintronic devices [1]. Diluted magnetic semiconductors (DMS) are the most interesting systems found to be for spintronic applications because magnetic ions doped materials are more effective than metal oxide systems. i.e., the magnetic ion modifies electron transport in the host semiconductor systems. It is well known that the paramagnetic ions (Fe, Mn and Co) in the tetrahedral semiconductor systems that provide the magnetic properties of that system [2]. Especially, in Co-doped CdS thin films Co^{2+} ions gives rise to a stable soft ferromagnetic coupling via a superexchange mechanism. The cobalt doped CdS have been proposed to be applicable in solar cells, diode sensors [3] and spintronic [4, 5].

In this perspective, the $Cd_{1-x}Co_xS$ thin films are prepared by several chemical methods such as sputtering [6], spray pyrolysis [7], chemical bath deposition [8] and electro-deposition [9]. Of these methods, chemical bath deposition (CBD) is simple and economic. In addition, it provides the suitable way to control the thickness and transparency of thin film with ease.

2 Experimental work

The glass substrate used for film deposition is glass slides, which were first cleaned with distilled water in order to remove the impurities and residuals from their surfaces, followed by rinsing in chromic acid for 1 day. Then the substrates were washed repeatedly with deionized water and finally cleaned using ultrasonic agitation with distilled water for 15 min then dried.

✉ S. Saravanakumar
  saranphys529@gmail.com

[1] Department of Physics, Sree Sevugan Annamalai College, Devakottai, Tamilnadu, India

[2] Department of Physics, Arumugam Pillai Seethai Ammal College, Thiruppattur, Tamilnadu, India

[3] Department of Physics, Pope's College, Sawyerpuram, Tamilnadu, India

[4] Department of Physics, Srinivasa Ramanujan Centre, SASTRA University, Kumbakonam 612001, Tamilnadu, India

CdS films were prepared from cadmium chloride and thiourea by chemical bath deposition technique. The reagents were used in aqueous of $CdCl_2 \cdot 2H_2O$, thiourea $[CS(NH_2)_2]$, ammonium chloride, ammonia and EDTA. In the reaction bath, 30 ml of 1 M ammonia solution was added to 7.5 ml of 0.05 M $CdCl_2 \cdot 2H_2O$, 10 ml of 0.1 M ammonium chloride. To the resulting mixture was added 7.5 ml of 1 M thiourea and 5 ml of 0.6mM EDTA to make up bath solution. Cobaltous chloride ($CoCl_2 \cdot 6H_2O$) was added for appropriate condition. The pH of the solution is kept at 11. The cleaned substrate was vertically inserted in the bath containing reaction mixture. The solution was maintained under constant magnetic stirring during the deposition at a temperature of 80 °C and deposition was allowed to settle for an hour. After the deposition process, the films were taken out from the bath and immediately rinsed with water and finally dried. After complete drying, the films were annealed at 350 °C for 1 h. The thicknesses of the films were found to be approximately determined by weight loss method. As-prepared samples were analyzed for the structural, morphological, elemental and magnetic properties has been studied by XRD, SEM and VSM methods. The proposed overall mechanism for the deposition of CdS is attributed to the following reactions;

$$Co^{2+} + CdCl_2 + (NH_2)_2 CS + 2OH^-$$
$$\rightarrow Co:CdS + H_2CN_2 + 2Cl^- + 2H_2O$$
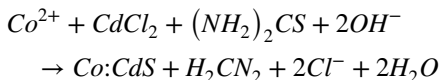
The thickness (t) of the films was calculated by using the weight gain method and these values were tabulated in the Table 1. The structural characterization of the films was carried out by X-ray diffractometer (PANalytical—PW 340/60Xpert PRO) with a CuKα radiation source (wavelength: 1.5418 Å). The chemical compositions and present bonding types on the surface and near-surface region of the films was examined by X-ray photoelectron spectroscopy (XPS) realized by a UNISPECS ESCA system equipped with a Mg Kα X-ray radiation source of 1253.6 eV-energy. The surface morphology and film composition were carried out by an analyzer setup attached to scanning electron microscope (Zeiss). The room temperature ferromagnetism was performed in a vibrating sample magnetometer (VSM) (Lakeshore Model 74035). The results are presented.

3 Results and discussion

3.1 Structural analysis

The X-ray diffraction patterns of $Cd_{1-x}Co_xS$ (x = 0, 0.05 and 0.1 M) films are shown in Fig. 1a, b and c, respectively. The diffraction peaks showed that the films have polycrystalline nature with hexagonal wurtzite structure with (0 0 2) preferential orientation, irrespective of the Co doping content, which indicates that the incorporation of Co into the Cd sites has not altered the preferential growth [10]. The other peaks observed at 2θ = 24.8°, 26.5° and 28.2° can be indexed to (1 0 0), (0 0 2) and (1 0 1) planes of $Cd_{1-x}Co_xS$ (x = 0, 0.05 and 0.1 M) films which is indexed using JCPDS standard pattern [11]. No diffraction peaks corresponding to Co metal or other impurity phases were observed in XRD diffraction patterns.

In this study can confirmed the formation of the $Cd_{1-x}Co_xS$ films. The predominance of the (0 0 2) plane in all the films clearly shows that the growth of the CdS structure, such that the c-axis is perpendicular to the surface of the substrate. The crystallite size (D) of CdS films is calculated using the Scherrer formula [12],
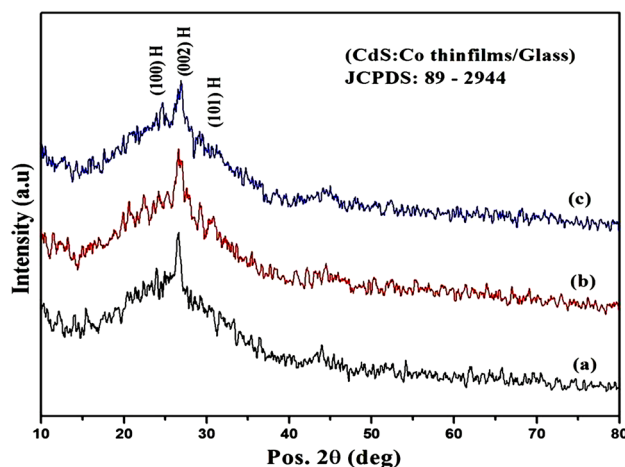
$$D = \frac{0.9\lambda}{\beta \cos \theta}$$

Fig. 1 X-ray diffraction pattern of $Cd_{1-x}Co_xS$ thin films obtained at various Co concentrations *a* x = 0, *b* x = 0.05 and *c* x = 0.1 M

Table 1 Structural, optical and magnetic properties of $Cd_{1-x}Co_xS$ (x = 0, 0.05 and 0.1 M) films

Co concentrations (x) (M)	Thickness (t) (µm)	Crystallite size (D) (nm)	Dislocation density (δ) (lines/m)^2	Strain (ε)	Bandgap (E_g) (eV)	Magnetic saturation (M_S) ($\times 10^{-6}$) (emu)	Magnetic rententivity (M_R) ($\times 10^{-6}$) (emu)	Magnetic coercivity (H_C) (Oe)
0	0.52	29	1.28	0.017	2.40	–	–	–
0.05	0.44	22	2.07	0.026	2.31	–	–	–
0.1	0.38	18	3.09	0.082	2.27	26.31	3.09	104.8

where λ is the wavelength of the X-ray used (1.5406 Å), β is the full width at half maximum of the strongest peak, and θ is the Bragg angle.

The crystallite size of the undoped and Co-doped CdS films was presented in the Table 1. The dislocation density (δ) is defined as the length of dislocation lines per unit volume of the crystal [13]. This was calculated from the following formula,

$$\delta = {}^1\!/_{D^2} \qquad (1)$$

$$\varepsilon = \frac{\beta \cos \theta}{4} \qquad (2)$$

Figure 2, shows the variation of dislocation density (δ) and strain (ε) values of undoped and Co-doped CdS thin films with respect to Co concentration. The crystallite size gradually decreased from 29 to 18 nm with the increased Co concentration [14]. In general, the crystallite size decreased with increased Co content, this is due to the lowest ionic radius of Co compared to Cd ions. The substitution of Co^{2+} (0.74 Å) ions at Cd^{2+} (0.97 Å) sites and difference of their ionic radii may be responsible for lattice defects with Co content. The strain increases indicating an increase in lattice defects in the CdS structure [15]. Hemathangam et al., suggested the increase of strain causes the decrease of lattice parameters and average crystallite size. In addition, this increase of strain is responsible for the broadening of diffraction peaks [16]. The above mentioned all the commends well matched within the present work. Similarly, the dislocation density values increased due to the increased dopant Co concentrations [17].
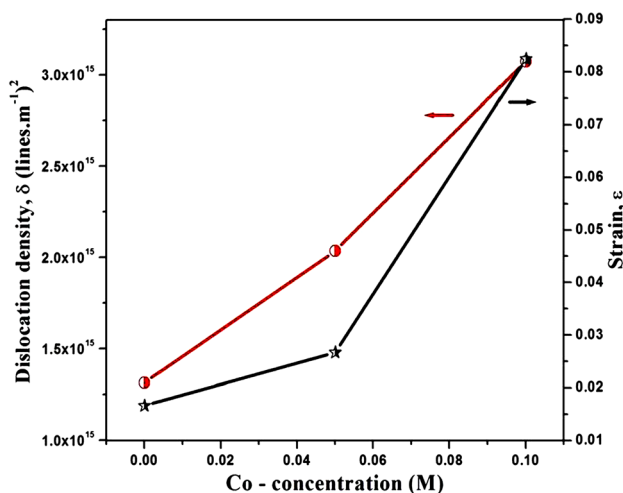
3.2 XPS analysis

XPS measurement is carried out to study the presence of chemical compositions of thin films. The full scan XPS spectrum is carried out in the range of 0–1200 eV for Co-doped CdS films is shown in Fig. 3a. The presence of peaks of Cd $2p_{3/2}$, Cd $2p_{1/2}$, Cd $3d_{5/2}$, Cd $3d_{3/2}$, Cd 4d, S 2s, S $2p_{3/2}$ and Co 2p centered at 619.8, 653.1, 404.9, 411.3, 11.3, 225.5, 161.7 and 773.8 eV were recorded respectively. The C 1s peak is deconvoluted into three components corresponding to C–H, C–OH and C=O which would correspond to organic species from the solution/from the air and is also shown in Fig. 3b. The O 1s peak is obtained at 534 eV which corresponds to the formation of $Cd(OH)_2$. The detailed spectrum of Cd 3d is shown in Fig. 3c which confirmed that the spin energy separation between Cd $3d_{5/2}$ and Cd $3d_{3/2}$ peaks is 6.4 eV [18]. The detailed spectrum of S $2p_{3/2}$ is shown in Fig. 3d and it has two main S 2p peaks. The first peak corresponds to CdS (161.8 eV) while the second peak is attributed to S–S peak (163.2 eV) and a small fraction of photoelectron peak of Co–S bonding is also in good agreement with the CoS_2 (162.4 eV) [19, 20]. The Co 2p peak is attributed to 778.7 eV [21]. The measured Co doped molar ratio is about 6.3%. Therefore the calculated atomic concentration of Cd and S is 58.6 and 41.4% respectively.

3.3 Morphological and compositional analysis

Figure 4a–c are the surface morphologies of undoped and Co doped CdS thin films, which depicts the deposited films are polycrystalline in nature and deposition covers the substrate well. In deposited film was very dense with few observable voids or grain boundaries. The morphology is contained cauliflower like grains typical of chalcogenides. The films have less defined grain boundaries under this magnification as Co is doped in Fig. 4b. The morphology is resembled a uniform amorphous layer embedded with small uniform sized grains. However, when Co concentrations are increased the morphology revealed a considerable change. The embedded layers tend to form spherical grains agglomerated as shown in Fig. 4c.

The EDAX spectra of pure and Co-doped CdS films are given in Fig. 5a–c, which shows that undoped CdS film contain the Cd and S elements only. The increase in Co concentrations has been obtained as the bath compositions are changed, whereas the doped films contain the Cd, S and Co elements as it has been expected. In Fig. 5d, the deviation of the S/(Cd + Co) ratio is found to be reduced in Co (0.1 M) doped CdS films and the difficulty in preparing sulfur deficiency free CdS films can be overcome by the addition of dopant concentration of the cationic solution [22].
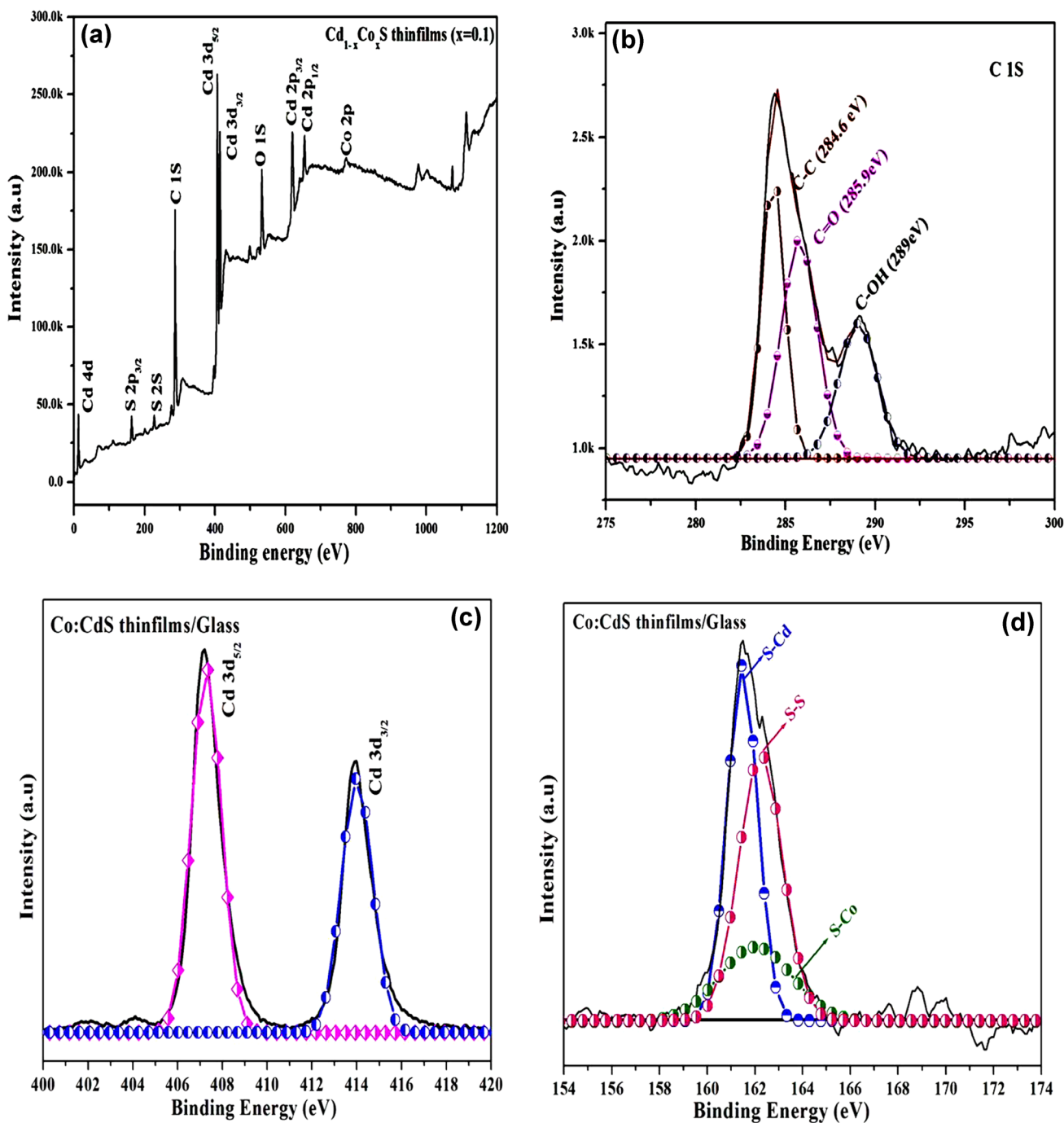

Fig. 2 The dislocation density and strain values for $Cd_{1-x}Co_xS$ thin films (x = 0 to 0.1 M)

Fig. 3 **a** XPS survey spectrum for Co-doped CdS thin films, **b** C 1s photoelectron peak, **c** Cd 3d doublet photoelectron peak and **d** S 2p photoelectron peak for CdCoS thin films

3.4 Optical studies

The optical absorption and transmittance spectra of all the samples are investigated between wavelength range 400–1100 nm and these are shown in Fig. 6a, b respectively. From the absorption spectra Fig. 6a, it observed that the absorption edge of $Cd_{1-x}Co_xS$ (x = 0.1 M) film is

blue shifted when compared with that of pure CdS films. This blue-shift is mainly attributed to a strong quantum confinement effect caused by the reduction in particle size [23]. The Optical transmittance of the CdS thin films is increased from 35 to 65% with Co doping. In the visible region, the transmittance of Co-doped films is lower than undoped CdS films due to the creation of oxygen vacancies
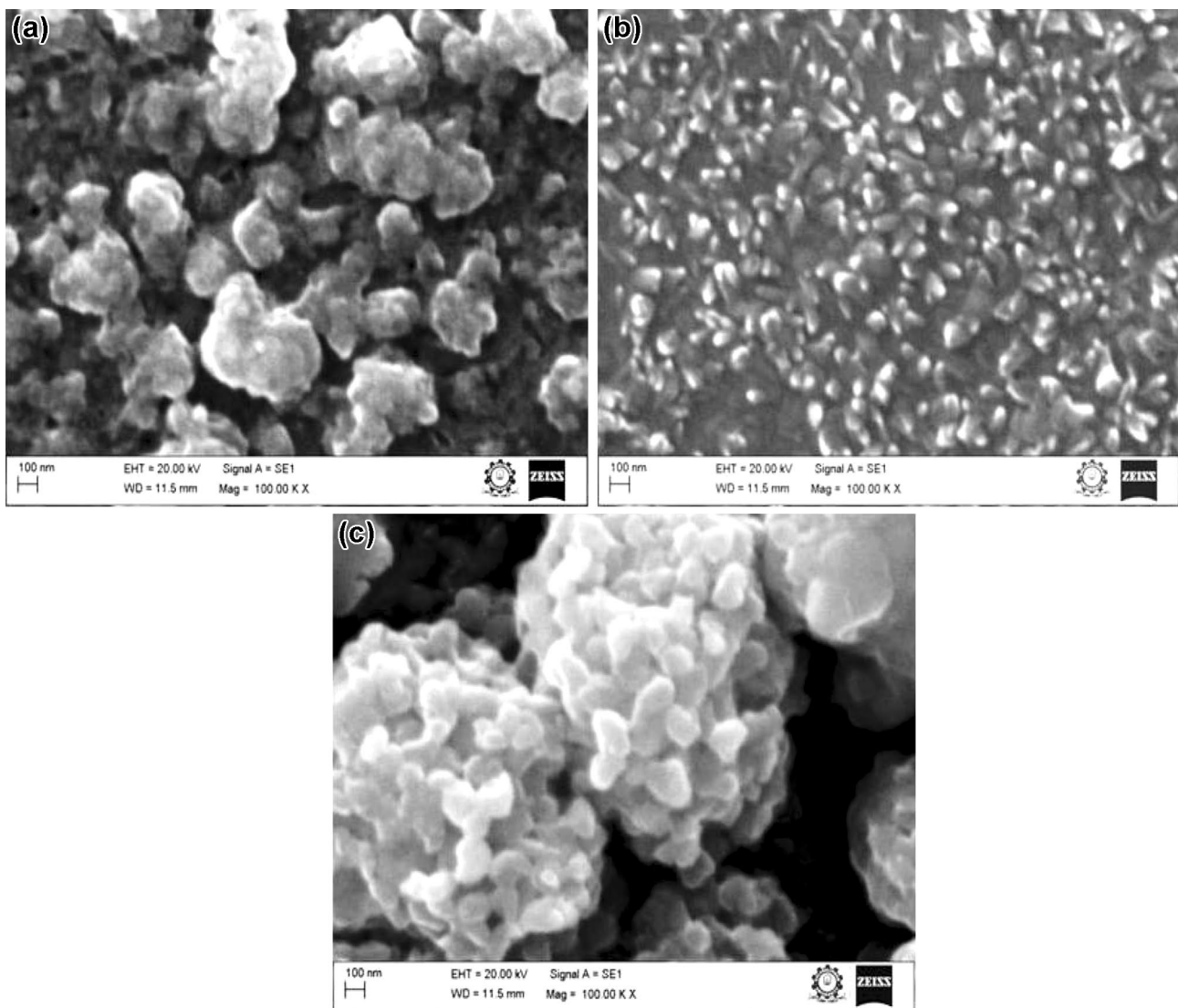
Fig. 4 SEM images of $Cd_{1-x}Co_xS$ films **a** x = 0, **b** x = 0.05 and **c** x = 0.1 M

and light scattering at the grain boundaries. The semiconductor band gap (E_g) of the film was calculated using the Tauc plot equation [24],

$$(\alpha h\nu) = A\left(h\nu - E_g\right)^n \tag{3}$$

where α is the absorption coefficient, h is Planck constant, A is a constant and ν is the photon frequency. The variation of $(\alpha h\nu)^2$ as a function of $h\nu$ is shown in Fig. 6c, the value of the band gap E_g is given by the intercept of the straight line with the energy axis. The obtained band gap value of this figure was listed in Table 1. The band gap of the Co doping CdS samples is decreased from 2.4 to 2.27 eV. The decrease band gap of samples can be due to the substitution of Co^{2+} ions into the host card lattice site. The decrease in

band gap could be arisen from increasing grain size and the improvement of crystallinity [25]. The bandgap of Co doped CdS samples decreased due to the sp-d exchange interaction between the electrons in CdS and localized electrons of Co^{2+} with Co doping. The decrease in bandgap of the samples can be due to the influence of various factors such as grain size, carrier concentrations and lattice strain. The decrease in bandgap can be arisen from increasing the grain size and the improvement of crystallinity. Also, the band gap can be decreased by increasing tensile stress depended on reducing lattice parameter [26]. The variation of extinction coefficient and refractive index (n) of undoped and Co-doped films as a function of Co concentrations in Fig. 6d.
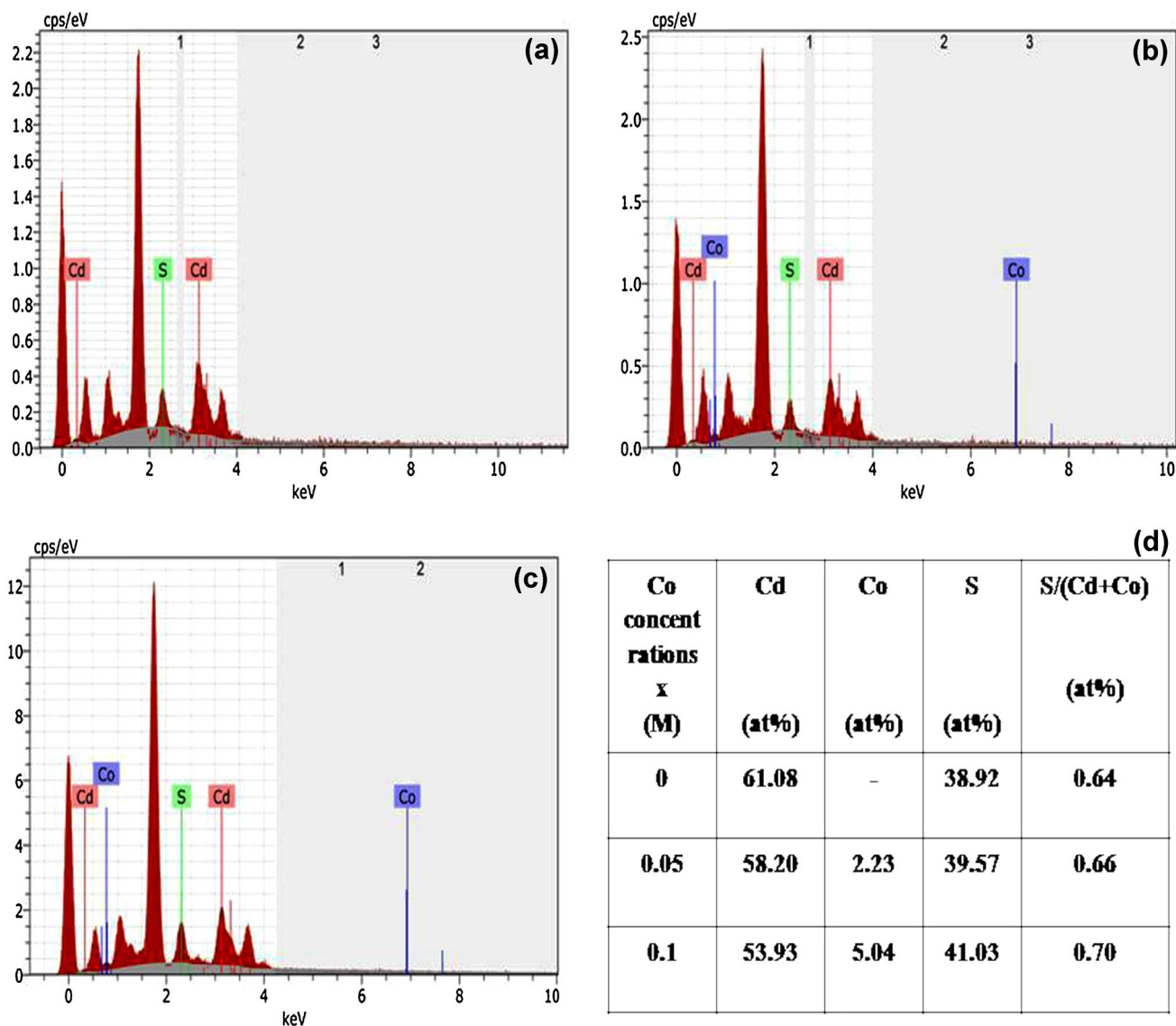
Fig. 5 EDX spectra of $Cd_{1-x}Co_xS$ films **a** x = 0, **b** x = 0.05, **c** x = 0.1 M and **d** calculated element values with S/Cd ratio

3.5 Magnetical studies

Figure 7, shows Co-doped CdS films exhibited the room temperature soft ferromagnetic properties by the variation of magnetization as a function of magnetic field. The saturation magnetization (M_s) strongly depends on the dopant concentration of the films. This M_s was probably caused by an increase electrons which induced more efficient ferromagnetic couplings between doped Co^{2+} ions with the host CdS [27]. i.e., Co^{2+} doped CdS thin films give rise to a stable soft ferromagnetic coupling via a superexchange mechanism in the sp-d electrons exchange interactions between sp electrons of CdS and d—electrons of Co^{2+} [28, 29]. All the calculated magnetic values were tabulated in Table 1.

4 Conclusion

The samples of $Cd_{1-x}Co_xS$ (x = 0, 0.05 and 0.1 M) films were prepared successfully by CBD method. From XRD data, it is confirmed that all samples are in the hexagonal CdS structure. The crystallite size of the films has been calculated by Debye Scherer's equation. It is observed that the average crystallite size decreases from 29 to 18 nm with increased Co content. From the XPS studies; a very small amount of Co atoms is found chemically bonded to S atoms and the Cd atoms present on the surface are oxidized to Cd^{2+} states. Therefore, Cd atoms on the surface of the films are found to be bound either to S atoms or O atoms. Although Cd-S bindings are mostly obtained in the Co-doped films. SEM images showed that
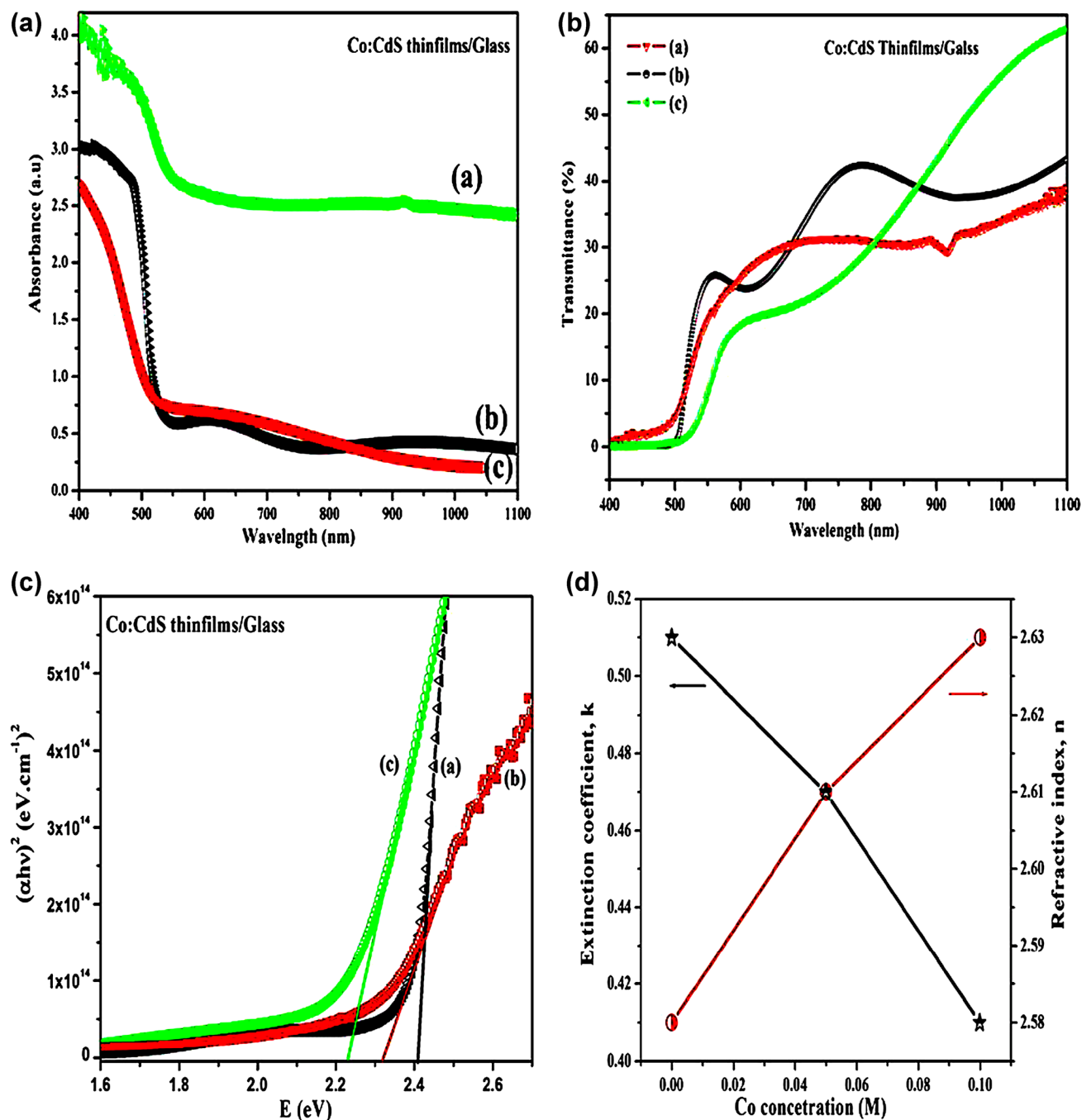
Fig. 6 a Optical absorption spectra, **b** transmittance spectra, **c** the Tauc plot for bandgap and **d** extinction coefficient and refractive index of the $Cd_{1-x}Co_xS$ films for $x = 0$ (sample-**a**), $x = 0.05$ (sample-**b**) and $x = 0.1$ M (sample-**c**)

the deposition produces varied morphologies. Energy dispersive X-ray study confirmed the presence of Cd, S and Co in the films. The UV–Vis. Spectra showed the direct band gap energy (E_g) is decreased from 2.4 to 2.27 eV with increasing Co content from 0 to 0.1 M. The Co-doped $Cd_{1-x}Co_xS$ ($x = 0.1$ M) films have shown the soft RT ferromagnetic behavior. This DMS material is mainly used for spintronic applications.

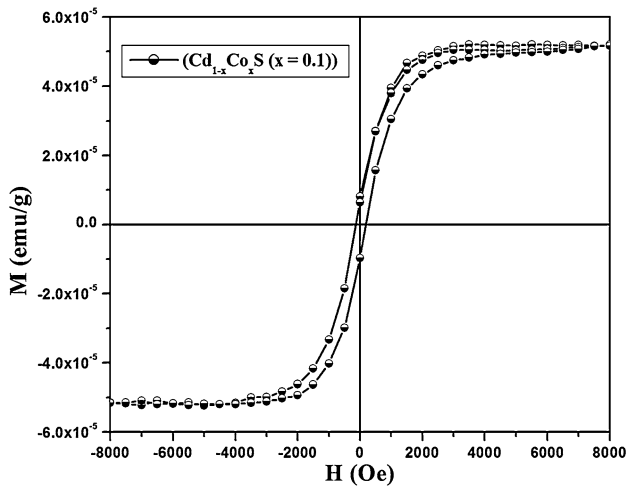**Fig. 7** VSM images for $Cd_{1-x}Co_xS$ (x = 0.1 M) thin films

References

1. S.S. Talwatkar, A.L. Sunatkari, Y.S. Tamgadge, V.G. Pahurkar, G.G. Muley, J. Nanostruct Chem **5**, 205 (2015)
2. K. Liu, J.Y. Zhang, X. Wu, B. Li, B. Li, Y. Lu, X. Fan, D. Shen, Phys. B **389**, 248 (2007)
3. E. Bacaksiz, M. Tomakin, M. Altunbas, M. Parlak, M. Colakoglu, Phys. B **403**, 3740 (2008)
4. S.C. Ezugwu, P.U. Asogwa, F.I. Ezema, R.U. Osuji, J. Non-Oxide Glasses **2**, 121 (2010)
5. U. Alvera, E. Bacakszb, E. Yanmaz, J. Alloys Compd. **456**, 6 (2008)
6. D.B. Fraser, H. Melchior, J. Appl. Phys. **43**, 3120 (1972)
7. B.K. Gupta, O.P. Agnihotri, A. Raza, Thin. Sol. Films **48**, 153 (1978)
8. S. N. Sahu, S. Chandra, Solar Cells **22**, 163 (1987)
9. G. Sasikala, R. Dhanasekaran, C. Subramanian, Thin Solid Films **71**, 302 (1997)
10. N. Mishack, Nabuchi, Chinedu and E. Ekuma. Chalcogenide Lett. **7**, 31 (2010)
11. JCPDS Card No 89 - 2944
12. B.D. Cullity, *Elements of X-ray Diffraction* (Addison-Wesley Publishing Company, Inc., Reading, 1978)
13. G.K. Williamson, R.E. Smallman, Philos. Mag. **1**, 34–46 (1956)
14. S. Thanikaikarasan, T. Mahalingam, M. Raja, T. Kim, Y.D. Kim, J. Mater. Sci. **20**, 727–734 (2009)
15. S. Kumar, N.S. Negi, S.C. Katyal, P. Sharma, V. Sharma, J. Magnet. Mag. Mater. **367**, 1–8 (2014)
16. S. Hemathangam, G. Thanapathy, S. Muthukumaran, J. Mater. Sci. (2016). doi:10.1007/s10854-015-3955-6
17. T. Mahalingam, R. Mariappan, V. Dhanasekaran, S.M. Mohan, G. Ravi, J.P. Chu, Chalco. Lett. **7**(12), 669–677 (2010)
18. M. Marychurch, G.C. Morris, Surf. Sci. **154**, L251 (1985)
19. E. Agostinelli, C. Battistoni, D. Fiorani, G. Mattogno, M. Nogues, J. Phys. Chem. Solids **50**, 269 (1989)
20. X.R. Yu, F. Liu, Z.Y. Wang, J. Y. Chen, Electron Spectrosc. Relat. Phenom. **50**, 159 (1990)
21. G.C. Stevens, T.J. Edmonds, Less-Common Met. **54**, 321 (1977)
22. K. Ravichandran, N. Nisha Banu, V. Senthamil Selvi, B. Muralidharan, T. Arun, J. Alloys Compd. (2016). doi:10.1016/j.jallcom.2016.06.164
23. M. Thambidurai, N. Muthukumarasamy, S. Agilan, N. Murugan, S. Vasantha, R. Balasundaraprabhu, T.S. Senthil, J. Mater. Sci. **45**, 3254 (2010)
24. J. Tauc, R. Grigorovici, A. Vancu, Phys. Status A **15**, 627 (1966)
25. M. Tomakin, M. Altunbas, E. Bacaksiz, I. Polat, J. Mater. Sci. Semicon. Process. **14**, 120–127 (2011)
26. M. Tomakin, M. Altunbas, E. Bacaksiz, I. Polat, J. Mater. Sci. Semicon. Process. **257**, 120–127 (2011)
27. Y.D. Reddy, D.S. Reddy, B.K. Reddy, R.V.S.S.N. Ravikumar, D.R. Reddy, J. Alloys Compd. **470**, 12 (2009)
28. M. Elango, K. Gopalakrishnan, S. Vairam, M. Tamilselvam, J. Alloys Compd. **538**, 48 (2012)
29. P. Venkatesu, K. Ravichandran, J. Adv. Mater. Lett. **4**, 202 (2013)